Desalination and Water Treatment
www.deswater.com

doi: 10.1080/19443994.2015.1046151

57 (2016) 12302–12315
June

Taylor & Francis
Taylor & Francis Group

Study on adsorption behavior of Acid Orange 10 onto modified wheat husk

Sushmita Banerjee*, Ravindra Kumar Gautam, Amita Jaiswal, Pavan Kumar Gautam, Mahesh Chandra Chattopadhyaya

Environmental Chemistry Research Laboratory, Department of Chemistry, University of Allahabad, Allahabad 211002, Uttar Pradesh, India, Tel. +91 9305138819; Fax: +91 5322462393; emails: sushmita.bnerjee@gmail.com (S. Banerjee), ravindragautam1987@gmail.com (R.K. Gautam), amita_ecsl@rediffmail.com (A. Jaiswal), pavanchemau@gmail.com (P.K. Gautam), mahesh46auchem@gmail.com (M.C. Chattopadhyaya)

Received 16 January 2015; Accepted 23 April 2015

ABSTRACT

The present communication addresses the applicability of acid-modified wheat husk for the adsorptive removal of an anionic dye, Acid Orange 10 (AO-10) from aqueous solutions. The adsorbent was characterized by FTIR and SEM. The adsorption reached equilibrium within 30 min, and the percentage removal increased with contact time, adsorbent dosage, and ionic strength. Low pH condition enhances AO-10 sorption. The experimental data for kinetic study agrees with pseudo-second-order model. Detailed investigation of experimental kinetic data indicates that overall sorption rate is governed by film diffusion mechanism. The adsorption behavior followed a Freundlich adsorption isotherm with high correlation coefficient and low χ^2 values. The maximum adsorption capacity was found to be 31.25 mg/g. The results of thermodynamic study demonstrated that the adsorption process was spontaneous and exothermic in nature. Desorption studies revealed that the adsorbent could be reused for two successive trials without significant loss of sorption capacity.

Keywords: Acid Orange 10; Wheat husk; Kinetics; Mass transfer; Isotherm; Desorption

1. Introduction

Everyday millions of tons of wastewater have been generated world wide as a result of various house hold, agricultural, and industrial activities and their effluents thus comprises thousands of organic, inorganic, and biological pollutants. Dyes are one of the most common organic pollutants consumed largely by textile and printing industries as a result effluents discharged from these industries contaminated with dyes and have high chemical oxygen demand [1]. It has been reported that nearly 10–20% of the dyestuffs were always wasted during its application in various industrial processes and consequently the remaining unused portion were released directly into the nearby water bodies [2]. Color is one of the characteristics of an effluent which further indicates about the water quality. The presence of dyes in the wastewater can be easily discernable at minute level and its direct discharge depreciates recreational and esthetic value of the receiving water bodies [3]. Most of these dyes are toxic to aquatic life and drastically upset the normal functioning of the aquatic ecosystem by interrupting the passage of sunlight through the water which ultimately ceases photosynthetic activity [4]. Dyes exhibit toxicity and are potentially mutagenic and carcinogenic to humans [5]. It is therefore important to

*Corresponding author.

eliminate these colored nuisances from the waste streams before their discharge to receiving streams. However, complex structure of dye molecules makes them highly resistant to aerobic treatment, biological degradation, stable to light, and oxidizing agents thus its elimination from the waste stream is a highly challenging task [6]. Several conventional remediation techniques such as chemical coagulation, chemical oxidation, froth floatation, ion exchange, membrane filtration, precipitation, photocatalytic degradation, and reverse osmosis were used for the removal of dyes from industrial effluents, but suffered from various setbacks for instance incompetent, quite expensive, nonselective, and sludge generation requires special infrastructure and maintenance [7,8]. Among the proposed methods, removal of dyes by adsorption technology is regarded as one of the most accepted treatment method due to its simplicity, high efficiency, and equally effective for all types of dye species; adsorbent can be easily regenerated, simple operation with no problem of sludge generation. Moreover, adsorption process can be considered as promising treatment, especially if the adsorbent is abundantly available and inexpensive [8]. Range of adsorbents has been tested for its potential in adsorptive removal of the dyes molecules from the aqueous solutions among which activated carbon considered as the most appealing one due its high degree of effectiveness. However, certain limitations including high operation costs, time consumption, and high-cost of regeneration restrict large scale application of activated carbon [9]. In recent times, numerous approaches being explored to derive cheaper and effective adsorbent having competency comparable to activated carbon. In this perspective use of waste biomass as an adsorbent for water treatment open up new vista that offers economical treatment. Recently, many researchers have investigated the use of several low-cost adsorbent derived from various agricultural, industrial, and poultry wastes as an efficient alternate to decontaminate pollutants from wastewater [6–18]. However, direct utilization of the agricultural wastes as an adsorbent in its raw form leads to leaching of organic substances such as lignin, pectin, and tannin [19]. In order to minimize such problems chemical treatment of the adsorbent is required, which not only reduce the organic content but also enhances the surface area and adsorption capacity of the sorbent.

Present study utilizes wheat husk, agricultural, and abundantly available waste/byproduct for the removal of an anionic dye Acid Orange 10 (AO-10) from aqueous solutions. Nevertheless, several studies have been reported [20,21] using wheat husk as an adsorbent, but the removal of AO-10 using wheat husks has never been reported so far. AO-10 is a monoazo dye, and is extensively used as food colorant and in paper and textile industries. The dye reportedly causes genotoxicity in Swiss albino mice [22], anemia, reticytosis, splenomegaly in pigs [23], and also has been reported to be dangerous for humans as well [24]. This invokes urgent removal of the dye from aqueous solutions. The main objective of the present study is to explore the feasibility of perchloric acid treated wheat husk for the removal of AO-10 from aqueous solutions. The effects of process variables optimized include initial dye concentration, contact time, solution pH, and temperature. Kinetics of removal, isotherm. and thermodynamics of the process were also evaluated.

2. Experimental

2.1. Adsorbate

The anionic dye, AO-10 also known as Orange G having chemical formula of $C_{16}H_{10}N_2Na_2O_7S_2$ with FW of 452.37, was procured from Merck India (P) Limited, Mumbai. Stock solution of the test reagent was made by dissolving 1.0 g of dye in 1L of double-distilled water. The stock solution was further diluted with double-distilled water to obtain the standard solutions of 10, 25, 50, and 75 mg/L of the dye.

2.2. Adsorbent modification

After collection, wheat husk was washed liberally with distilled water to make it free from dust, and kept for drying in oven at 70˚C for 4 h. About 250 g of dried wheat husk was treated with 1% of perchloric acid in a ratio of 1:5 (wheat husk:perchloric acid) at 50˚C for 4 h. The treated wheat husk was filtered out, washed with distilled water, and kept in the oven for 24 h at 70˚C. The dried material was taken out of the oven and was stored in desiccators for further use.

2.3. Chemicals used

All the chemical reagents were of analytical grade and used as such without any further purification. The main chemicals used were HCl (Merck, Mumbai), NaOH (Merck, Mumbai), sodium dodecyl sulfate (SD fine chemical, Mumbai), NaCl (Merck, Mumbai), acetic acid (Merck, Mumbai), and double-distilled water (Merck, Mumbai).

2.4. Characterization of the adsorbent

The presence of functional groups in the sample was determined by FTIR spectra analysis. The spectrum was recorded at room temperature on FTIR spectrophotometer (FTLA-2000ABB, Canada) in the range of 4,000–500 cm^{-1} with a resolution of 2 cm^{-1}. Pellets were prepared with 13 mm die set by compressing an intimate mixture obtained by grinding 1 mg of the substance in 100 mg of KBr with mortar and pestle and applying an optimum pressure of nine ton using a 15 ton hydraulic pellet pressure (Kimaya Engineers, Thane).

The surface morphology of the adsorbent was analyzed through scanning electron microscope (Zeiss, Germany) at 5.0 kV accelerated voltage at a magnification of 250 ×.

2.5. Adsorption studies

The batch experiments were conducted in order to optimize various operating parameters that affect the adsorption process of AO-10 by modified wheat husk. To carry out batch adsorption studies, 100 mL dye solution of desired concentration was taken in 250 mL of Erlenmeyer flasks at a fixed temperature. The mixture was mechanically agitated at a constant speed of 200 rpm using water bath shaker (Mac-MacroScientific Works, Pvt. Ltd, New Delhi, India). The samples were withdrawn after predetermined time, and kept for 24 h for saturation. Thereafter, the adsorbent was separated from the solution by centrifugation using Remi centrifuge machine (Model-R-8CBL). The residual dye concentration was estimated in supernatant spectrophotometrically on double beam spectrophotometer (Model-2203 Systronics, Ahmadabad, India) over a wavelength range of 480 nm, which is the characteristic peak for AO-10.The effect of initial pH on the adsorption process was studied over a pH range of 2.0–10.0, being adjusted using 0.1 M NaOH or 0.1 M HCl. The adsorption isotherm experiments were carried out with dye solutions of different concentrations (10–75 mg/L) being agitated with the known amount of adsorbent (5.0 g/L) at different temperatures (303, 313, and 323 K) till the equilibrium was achieved. Adsorption kinetic investigations were carried out at different time intervals with four different initial dye concentration keeping temperature, pH, adsorbent dose, and agitation speed constant. The residual dye concentrations were analyzed from the calibration curve plotted between absorbance and concentration of each standard dye solution.

Blank experiments were also conducted using dye solution without adsorbent to ensure that no dye was adsorbed onto the containers and with adsorbent and water only to check that no leaching occurred from the prepared adsorbent, which would rather interfere with the measurement of dye concentrations on the spectrophotometer. All adsorption experiments were performed in triplicate and the mean values were taken for the data analysis.

3. Results and discussion

3.1. Characterization of adsorbent

The presence of surface functional groups was investigated via FTIR analysis of the raw, modified, and dye-loaded wheat husk. The FTIR spectra of raw wheat husk, acid-modified wheat husk, and dye-loaded wheat husk are displayed in Fig. 1(a)–(c). The spectra of the raw and modified adsorbent were measured within the range of 500–4,000 cm^{-1}. The figure displays some peaks are shifted or disappeared and some new peaks are also detected. All three spectra reveal a wide band at 3,200–3,600 cm^{-1} with maximum at 3,470 cm^{-1}, which can be ascribe to the stretching of hydroxyl group and adsorbed water [25], the intensity of hydroxyl peak indicates that the OH content of raw wheat husk is quite higher than that of modified form. The presence of band at 2,934 cm^{-1} can be corroborated to C–H stretching of methyl and methylene groups which after treatment are disappeared. The peak at around 1,635 cm^{-1} of raw adsorbent suggested the presence of amide group [26]; however, the peak position remains unaltered even after modification. The peak observed at 1,380 cm^{-1} due to vibration of $–CH_3$ in lignin another adjacent peak present at 1,311 cm^{-1} is related to bending

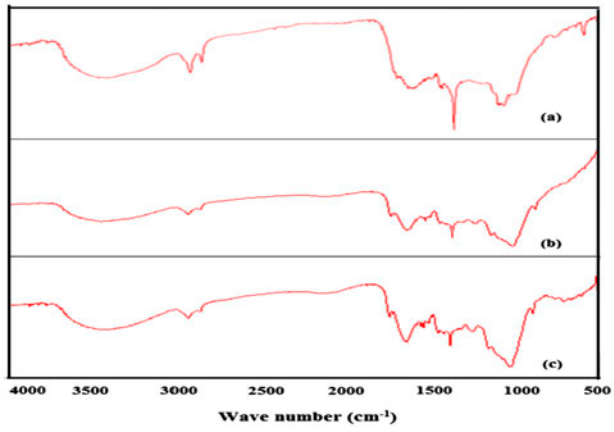

Fig. 1. FTIR spectra of (a) raw wheat husk, (b) modified wheat husk, and (c) AO-10 loaded wheat husk.

vibration of hydroxyl group or carbonyl group of cellulose these peaks shifted slightly after acid treatment. The peak visible at 1,252 $cm^{-1}$is due to stretching of C–O of acetyl groups in hemicelluloses after modification peak shifted little bit toward left side at 1,259 cm^{-1}. A less intense peak at 863 cm^{-1} allied to the planar bending vibrations of C–H or out of plane deformation of C–H and hydroxyl group in pyranoid rings of cellulose [27] and after modification weak shoulder is observed at 858 cm^{-1}. After chemical treatment (Fig. 1(b)), the presence of prominent peak at 1,631 cm^{-1} is observed due to stretching of C=C of benzene ring. This peak seems to be absent in raw wheat husk. Therefore, from the above description it can be concluded that acid treatment modifies the adsorbent appreciably. The spectra of dye-loaded adsorbent reflects that no significant change takes place in the adsorbent after dye adsorption which further implies that adsorbate–adsorbent interaction is purely physical in nature as there is no evidence of formation of any chemical bonding between the dye and sorbent.

The surface morphology of the adsorbent can be examined through SEM images. Fig. 2 represents the SEM micrographs of raw wheat husk and modified wheat husk. The raw wheat husk (Fig. 2(a)) comprises irregular surfaces with smooth features, whereas the acid-modified adsorbent (Fig. 2(b)) exhibits numerous well developed pores. These deeply grooved features are capable of accommodating large number of AO-10 ions.

3.2. Effect of chemical modification

The biological adsorbent in its raw form usually exhibits low sorption capacity due to the presence of organic molecules which may hinders attachment of dye ions on the adsorbent surface. This problem can be overcome by directing some chemical and physical treatment to the adsorbent. In the present study, wheat husk has been modified with different types of chemical reagents and the resultant material with highest sorption capacity for AO-10 was finally used for the experimental analysis. The following order was observed for various chemical treatments on the loading capacity of wheat husk as compared to its raw form. Raw (5.6) < EDTA (8.2) < $NaHCO_3$ (10.3) < $NaCO_3$ (11.5) < NaOH (12.4) < Boiling water (13.2) < $H_2C_2O_4$ (13.6) < CH_3COOH (15.2) < HNO_3 (22.9) < HCl (24.7) < H_3PO_4 (25.3) < H_2SO_4 (26.1) < $HClO_4$ (31.1). The results indicated that adsorption efficiency of the wheat husk got augmented remarkably from 5.6 to 31.1 mg/g after modification with perchloric acid. The increase in sorption capacity was probably due to removal of organic molecules as well as development of positive charge that resulted in enhanced interaction between anionic dye ions and positively charged sorbent surface.

3.3. Effect of contact time and initial dye concentration

Fig. 3 shows the effect of contact time on the percentage removal of AO-10. It can be seen that with

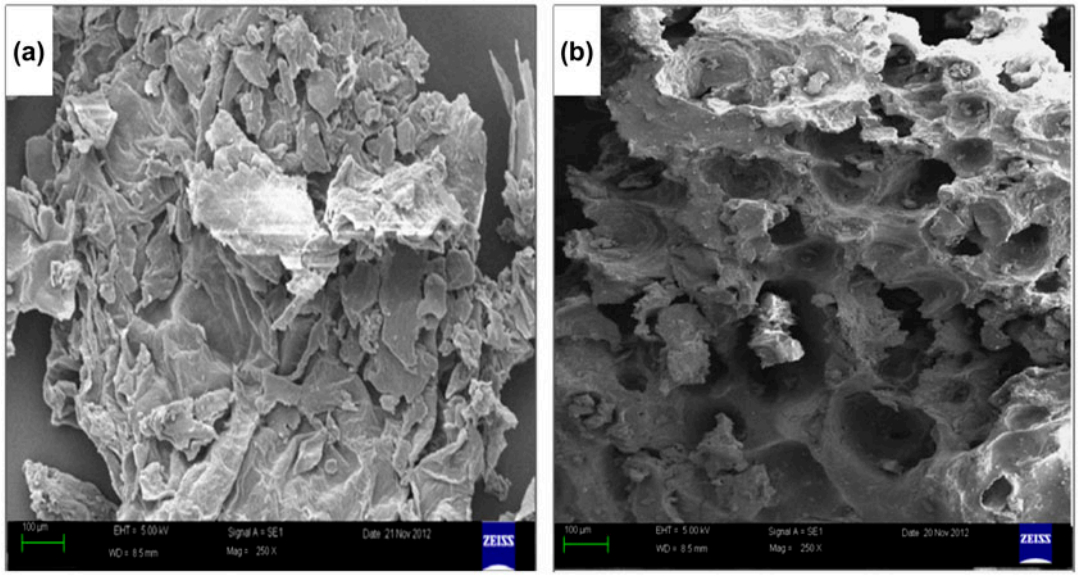

Fig. 2. SEM image at 250 × of (a) raw wheat husk and (b) modified wheat husk.

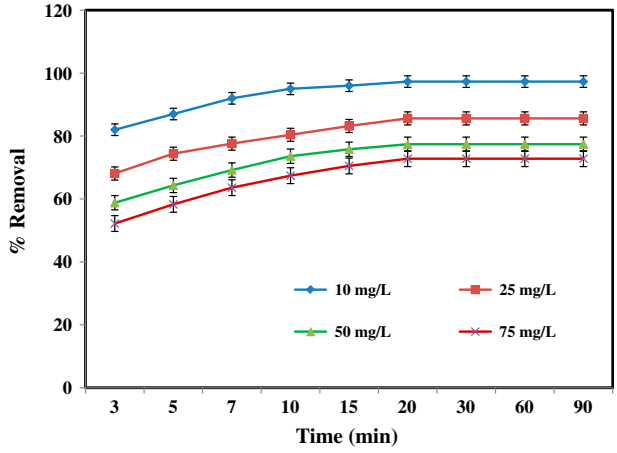

Fig. 3. Effect of initial dye concentration on percentage removal of AO-10 by modified wheat husk (agitation speed 200 rpm, adsorbent dose 2.5 g/L, temperature 303 K, pH 2.0).

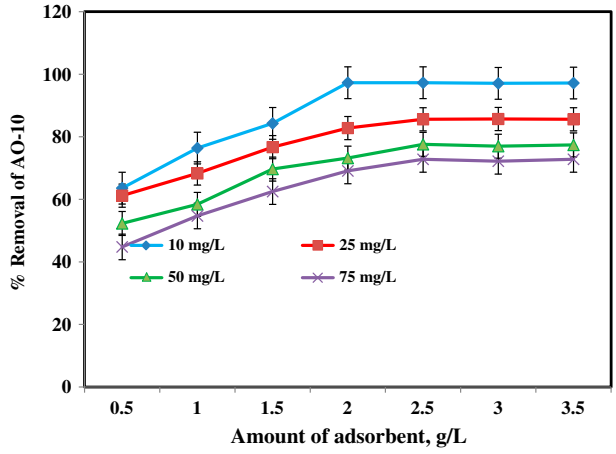

Fig. 4. Effect of adsorbent dose on percentage removal of AO-10 by modified wheat husk (agitation speed 200 rpm, temperature 303 K, pH 2.0).

the increase in contact time, the percentage dye removal also increases until the equilibrium is attained. More than 50% of dye removal takes place within first 5 min of contact time and complete dye saturation is observed within 30 min. It can also be seen that percentage removal of dye decreases with increase in initial dye concentration. At lower concentration (10 mg/L) maximum sorption of 97.3% was observed, whereas at higher concentration (75 mg/L) sorption percentage got decreased to 72.8%. This can be due to the fact that at low concentrations, less number of dye ions are able to interact easily with the largely available binding sites of the adsorbent but as the dye concentration increases, it becomes rather difficult for the dye ions to interact with the active sites as dye ions start competing for the active sites of the adsorbent. Moreover, all adsorbents have limited number of binding sites which tend to equilibrate at certain dye concentration [28].

3.4. Effect of adsorbent dose

The result for the adsorptive removal of AO-10 with respect to adsorbent dose is depicted in Fig. 4 over the range of 0.5–3.5 g/L. It is observed that percentage of dye removal increases with increase in sorbent dosage. The positive correlation can be observed between dye uptake and sorbent dosage, which may be attributed to increase in adsorbent surface area and greater availability of sorption sites [29]. Maximum dye removal is observed at 2.5 g/L of adsorbent dosage; however, further increase in dosage does not show significant removal. This may be due to saturation of all binding sites of the adsorbent with the dye ions and attainment of equilibrium between dye ions in the bulk and on the surface of adsorbent. Therefore, 2.5 g/L of adsorbent dosage was used in successive experiments.

3.5. Effect of temperature and contact time

Fig. 5 shows the adsorption profile of AO-10 vs. temperature as a function of contact time. The figure indicates that the sorption capacity of dye decreases with the increase in temperature. The sorption capacity remarkably declines from 3.84 to 2.52 mg/g with the increase in temperature from 303 to 323 K. The decrease in dye sorption capacity with the increase in temperature attributed to either weakening of the

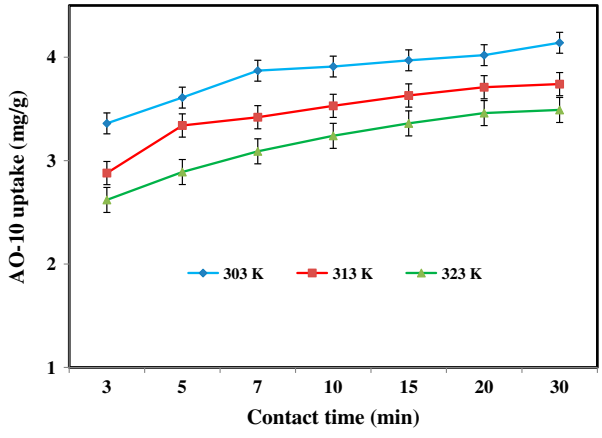

Fig. 5. Effect of temperature on uptake of AO-10 by modified wheat husk (agitation speed 200 rpm, initial dye concentration 10 mg/L, pH 2.0, adsorbent dose 2.5 g/L).

physical interaction between the dye ions and the active sorption sites [30] or may be due to the escaping tendency of dye ions from the solid phase and re-enter into the liquid phase due to enhanced mobility with the increase in temperature [31].

3.6. Effect of pH

Solution pH is one of the most prominent parameters controlling the uptake of dye ions from aqueous solutions. It influences the sorption process by altering the surface charge of the adsorbent as well as degree of ionization of the sorbate species. Change in solution pH affects the adsorptive process through dissociation of functional groups present on the adsorbent surface [32]. Prior to experimental analysis it has been ensured that change of the initial solution pH from pH 2.0 to 10.0 (Fig. 6) of dye solution has insignificant effect on λ_{max} of AO-10. As a result absorbance of the solutions was measured at precise wavelength of 480 nm. This observation indicates that change in solution pH doesn't alter the chemical structure of dye molecules and therefore, the removal of the dye results exclusively owing to adsorption process. It can be noticed (Fig. 6) that maximum dye removal takes place at a lower pH value of 2.0 and as the pH of solution is raised, the removal efficiency decreases significantly. This can be explained as at low pH, the adsorbent surface gets protonated and thus attracted anionic dye ions through electrostatic forces but as the pH of the solution is decreased, the adsorbent surface gets deprotonated which greatly resists the uptake of anionic dye ions due to existence of repulsive forces between dye anions and negatively charged active sites of the adsorbent. The mechanism of AO-10 adsorption under acidic condition can be represented by the following scheme, where Ce-OH represents adsorbent:

$$\text{Ce-OH} \xrightarrow{\text{pH} < 4\ \text{(protonation)}} \text{Ce-OH}_2^+ \quad (1)$$

$$\text{Dye} - \text{SO}_3\text{Na} + \text{H}_2\text{O} \xrightarrow{\text{dissociation}} \text{Dye} - \text{SO}_3^- + \text{Na}^+ \quad (2)$$

$$\text{Ce-OH}_2^+ + \text{Dye} - \text{SO}_3^- \xrightarrow{\text{electrostaticinteraction}} \text{Ce-OH}_2^+\text{SO}_3^- - \text{Dye} \quad (3)$$

The dye removal mechanism can also be explained on the basis of pH_{ZPC}. The pH_{ZPC} of the modified wheat husk is evaluated as 5.9. At $pH > pH_{ZPC}$ the adsorbent surface becomes negatively charged discouraging adsorption of anionic dyes. When $pH < pH_{ZPC}$, the surface of the adsorbent gets positively charged, thus favors sorption of negatively charged dye ions [33].

3.7. Effect of ionic strength

In an attempt to investigate the effect of ionic strength on removal efficiency of AO-10, the removal process has been carried out in the presence of anionic surfactant, sodium dodecyl sulfate (SDS), and NaCl. The presence of these salts affects the ionic strength of the solution by interfering with the electrostatic forces between the adsorbent and dye ions. It can be perceived from Fig. 7 that the dye removal

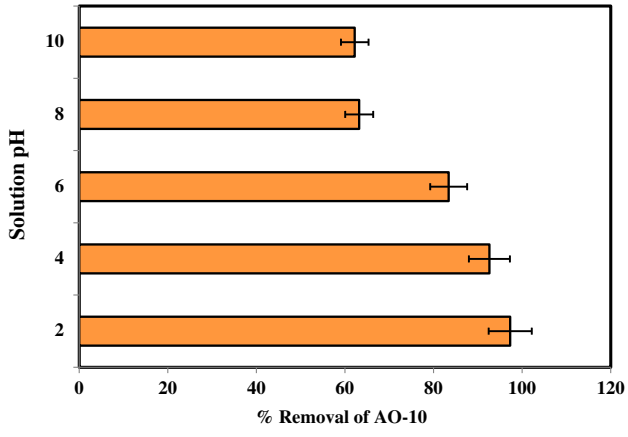

Fig. 6. Effect of solution pH on percentage removal of AO-10 by modified wheat husk (agitation speed 200 rpm, temperature 303 K, initial dye concentration 10 mg/L, adsorbent dose 2.5 g/L).

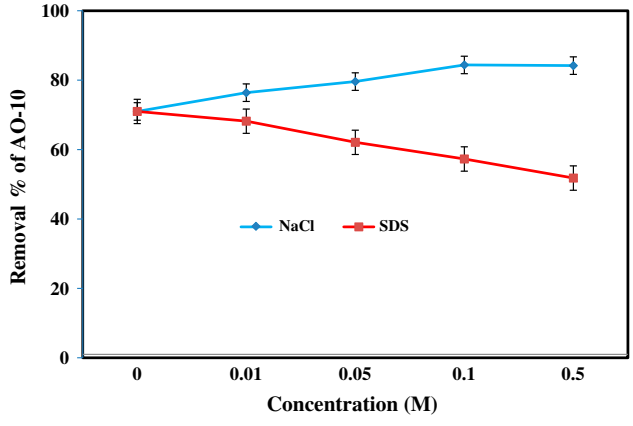

Fig. 7. Effect of ionic strength on percentage removal of AO-10 by modified wheat husk (agitation speed 200 rpm, temperature 303 K, initial dye concentration 10 mg/L, pH 7.0, adsorbent dose 2.5 g/L).

percentage increases from 71.2 to 84.4% in presence of NaCl, but decreases from 71.2 to 51.8% in presence of SDS at solution pH 7.0. This can be explained as at pH 7.0, adsorbent is negatively charged as pH_{ZPC} is 5.9 and the dye ions are also negatively charged, thus both species bear identical charges, when small amount of NaCl is added, the ionic strength increases which reduces the negative charges on the adsorbent surface, hence increased the electrostatic interaction between dye ions and surface active sites of adsorbent [34].

However, in case of SDS addition the decrease in removal percentage attributed to increased competition between negatively charged dye ions and anionic surfactant for active sites of the adsorbent.

3.8. Adsorption kinetics

In order to investigate the adsorption mechanism of AO-10 on modified wheat husk, the data were analyzed by pseudo-first-order, pseudo-second-order kinetic model and with intra particle diffusion model. The pseudo-first-order kinetic [35,36] model in linearized form can be expressed by the following equation:

$$\log\ (q_e - q_t) = \log q_e - (k_1/2.303)t \quad (4)$$

The pseudo-second-order kinetics [35,37] in linearized form can be expressed as:

$$t\ /\ q_t = 1/k_2 q_e^2 + 1/q_e t \quad (5)$$

Intraparticle diffusion model can be represented by the equation given by Weber and Morris [38]:

$$q_t = k_{id} t^{0.5} \quad (6)$$

where k_1 is the pseudo-first-order rate constant (min^{-1}) and k_2, pseudo-second-order rate constant (min g/mg) and q_e is the amount of dye adsorbed at equilibrium (mg/g), q_t is the amount of dye adsorbed at time t (mg/g), k_{id} is the intraparticle diffusion rate constant (mg/g $min^{0.5}$), and C (mg/g) is a constant.

The values of pseudo-first-order rate constants; k_1 and q_e were evaluated from the slope and intercepts of the plots of log (q_e-q_t) vs. t (figure not shown). The k_1 values, the correlation coefficients R^2, and theoretical and experimental sorption capacity q_e are given in Table 1. Low correlation coefficient values and wide variation in theoretical and experimental values of equilibrium sorption capacity indicate that the pseudo-first-order kinetic model is not suitable for the process of removal of the dye in present system. Therefore, pseudo-second-order kinetic model was used to represent the sorption kinetic data. The plot of t/q_t against t for different initial dye concentration is given in Fig. 8. The plots exhibit linearity with high correlation coefficient values of 0.99, additionally; the theoretical values were much closer to experimental values of equilibrium sorption capacity. The rate constant k_2 decreased from 0.662 to 0.0011 mg/g min (Table 1) as the initial concentration increased from 10 to 75 mg/L, indicating that the adsorption is dependent on initial concentration. Therefore, it can be inferred that AO-10 adsorption on modified wheat

Table 1
Kinetics parameters for AO-10 adsorption on modified wheat husks at different initial dye concentrations

	10 mg/L	25 mg/L	50 mg/L	75 mg/L
Pseudo-first-order model				
k_1 (min^{-1})	0.22	0.172	0.216	0.183
$q_{e\ (cal)}$ (mg g^{-1})	1.07	2.65	7.423	11.01
$q_{e\ (exp)}$ (mg g^{-1})	3.97	8.52	16.50	23.31
χ^2	2.11	4.04	5.02	6.49
R^2	0.961	0.977	0.986	0.977
Pseudo second order model				
k_2 (g mg^{-1} min^{-1})	0.662	0.793	0.013	0.011
$q_{e\ (cal)}$ (mg g^{-1})	4.12	8.748	15.48	21.84
χ^2	0.005	0.006	0.06	0.092
R^2	0.999	0.998	0.999	0.999
Intraparticle diffusion model				
$k_{id,}$ (mg/g.$min^{0.5}$)	0.195	0.405	1.112	1.813
I	3.07	6.205	10.17	13.05
R^2	0.936	0.980	0.985	0.988

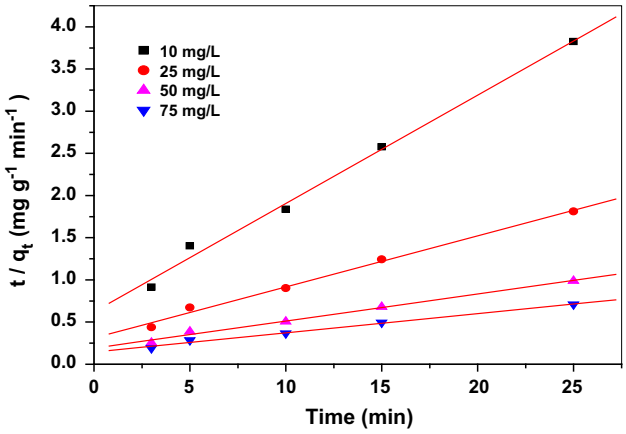

Fig. 8. Pseudo-second-order kinetic plots for adsorption of AO-10 at different initial dye concentration (adsorbent dose 2.5 g/L; pH 2; agitation speed, 200 rpm; temperature 303 K).

husk can be effectively represented by pseudo-second-order kinetic model, and the rate-limiting step of the sorption process may be controlled through sharing or exchanging of electrons between sorbent and sorbate [39].

The sorption kinetic data were further analyzed by intraparticle diffusion model to investigate the rate-limiting step of the sorption process. If the Weber-Morris plot of q_t against $t^{0.5}$ result in a linear relationship and the line passes through origin, then intraparticle diffusion will be rate-determining step. However, if the data exhibit multi-linear plots, then two or more steps influence the sorption process [40]. In this study, the plots (Fig. 9) exhibit linearity but do not pass through the origin suggesting that

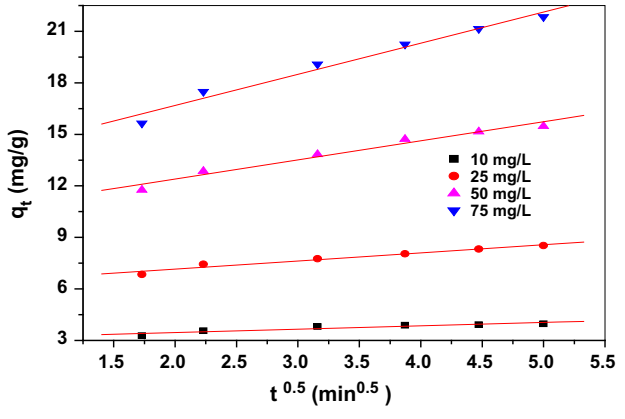

Fig. 9. Intraparticle diffusion profile for adsorption of AO-10 at different initial dye concentration (adsorbent dose 2.5 g/L; pH 2; agitation speed, 200 rpm; temperature 303 K).

intraparticle diffusion is not the rate-limiting step. The dye adsorption process must be driven by film diffusion mechanism. Meanwhile, perusal of parameter k_{id} exhibits increasing trend with the increase in initial dye concentration, this behavior may be attributed to the increased adsorption driving force offered by dye molecules leading to enhanced AO-10 diffusion rate. The increase in I values (Table 1) indicates the increase in boundary layer thickness as the initial dye concentration increased from 10 to 75 mg/L.

3.9. Mass transfer study

The study of mass transfer is important as it is helpful in predicting the removal rate of pollutants from aqueous phase and its simultaneous accumulation over solid surface. A well-known mathematical model was used to calculate mass transfer coefficient, β_L, using following equation [41]:

$$\ln\{(C_t/C_0 - 1/(1+mk)\} = \ln\{(mk\ /\ (1+mk) - (1+mk)\ /\ mk)\}\beta_L S_s t \quad (7)$$

where C_t is the concentration of adsorbate after time 't' (mg/L); C_0 is the initial concentration of the adsorbate (mg/L); k is the Langmuir constant obtained by multiplying adsorption capacity Q^0, and energy parameter$b$; β_L is the mass transfer coefficient, cm/s; m is the mass of the adsorbent per unit volume of the adsorbate solution (g/L). It is given by

$$m = M/V \quad (8)$$

S_s is the specific surface area of the adsorbent (m^2/g) and is calculated as:

$$S_s = 6\ m\ /\ (d_p \rho_p\ (1 - \in_p)) \quad (9)$$

where d_p is the particle diameter (cm); ρ_p is the bulk density of the adsorbent estimated as 0.37(g/cm^3); and ε_p is the porosity of the adsorbent particles in this study it is taken as 0.7. The values of mass transfer coefficient (β_L) were determined from the slopes of the linear plot of ln $[(C_t/C_0) - 1/(1+mk)]$ vs. t (Fig. 10). The calculated values of mass transfer coefficient at different temperature were presented in Table 2. The β_L values were found to decrease with temperature indicate exothermic nature of the process. In addition, the magnitude of β_L values obtained is in order of 10^{-5} cm/s further suggested that the transfer rate of

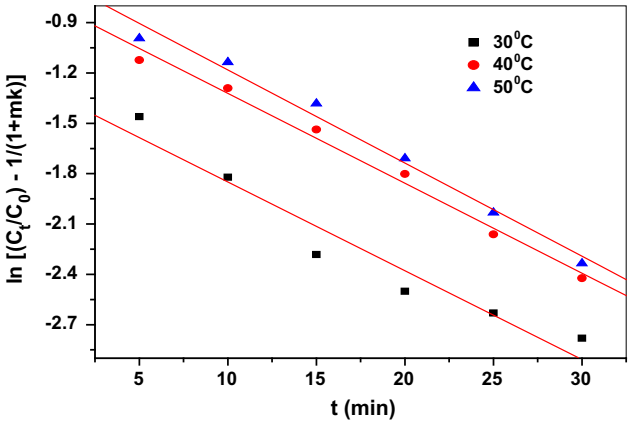

Fig. 10. Mass transfer plots for adsorption of AO-10 at different temperatures.

Table 2
Mass transfer coefficient (β_L) and effective diffusion coefficients for adsorption of AO-10 at different temperatures

Mass transfer	303 (K)	313 (K)	323 (K)
$\beta_L S_S$ (sec^{-1})	0.0545	0.0514	0.0405
$\beta_L \times 10^{-5}$ (cm s^{-1})	7.2	6.6	5.2
R^2	0.883	0.979	0.984
Boyd Kinetic model	303 (K)	313 (K)	323 (K)
B (sec^{-1})	0.078	0.64	0.062
$D_i \times 10^{-6}$ (cm^2 s^{-1})	9.52	7.79	7.53
R^2	0.922	0.958	0.988

dye molecules from bulk to solid surface is quite rapid enough. Therefore, the adsorbent can be effectively used for fast removal of dye from polluted water.

3.10. Rate expression and data treatment

In order to determine the overall process that governs the adsorbate–adsorbent interaction and removal rate of pollutants from liquid phase, it is required to further interpret the sorption kinetic data with a mathematical model given by Boyd et al. [42]. The Boyd expression given as follows:

$$F = 1 - \frac{6}{\pi^2}\sum_{n=1}^{\infty}\frac{1}{n^2}\exp\left[\frac{-D_i t\pi^2 n^2}{r_0^2}\right] \quad (10)$$

$$F = 1 - \frac{6}{\pi^2}\sum_{n=1}^{\infty}\frac{1}{n^2}\exp\left[-n^2 Bt\right] \quad (11)$$

where F is the fractional attainment of equilibrium at time t and calculated as:

$$F = q/q_{\infty} \quad (12)$$

where q and q_α represents the amount adsorbed (mg/g) at any time t and at infinite time (in the present study 30 min.), D_i is the effective diffusion coefficient of dye ions in adsorbent phase, r_0 is the radius of the adsorbent particle which was assumed as spherical and n is an integer. The value of B_t calculated for each value of F using Richenberg table [43]. The plot of B_t vs. t provide useful information in predicting the nature of sorption process which may be controlled either by film or pore diffusion. If the plot is linear and passes through the origin, then pore diffusion governs the sorption process and if the plot deviates from linearity, then film diffusion is considered to be rate-limiting step. The calculated B_t values were plotted against time t at different temperature shown in Fig. 11. The obtained Boyd profile shows that the plots for all temperature deviate significantly from linearity and are not well correlated by the fit. This clearly suggests that film diffusion is the rate-controlling step. This can also be substantiated by calculating the effective diffusion coefficient (D_i) values using following equation:

$$B = \pi^2 D_i / r^2 \quad (13)$$

where r represents the radius of the particle which is in the range of 0.6–1.0 mm (calculated by sieve analysis) and an average of two 0.075 cm was used in the calculation. B can be determined from the slope of Boyd plot. The calculated values of D_i presented in

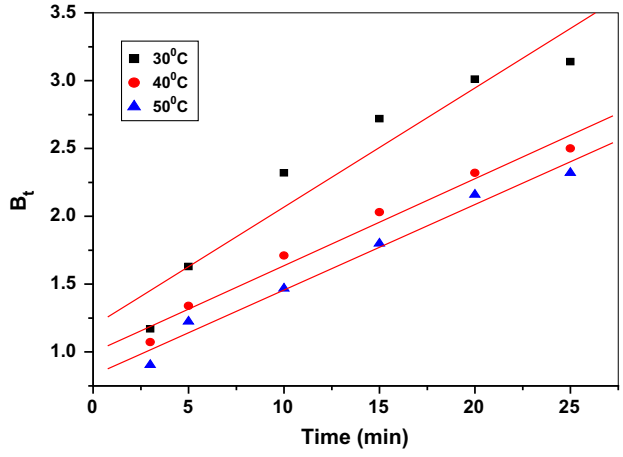

Fig. 11. Plot of time vs. B_t for AO-10 adsorption at different temperatures.

Table 3, it can be seen that the values of D_i increase with the decrease of temperature indicating lower temperature favors rapid transport of dye ions from bulk phase to adsorbent phase. Furthermore, according to Goel et al. [44], film diffusion is the rate-limiting step when the values of D_i approximated in the range of $10^{-6}-10^{-8}$ cm/s and for pore diffusion process, the D_i should be in the range of $10^{-11}-10^{-13}$ cm/s. Experimental data reveals that the adsorption of AO-10 on modified wheat husk was governed by film diffusion mechanism as the effective diffusion coefficient evaluated in the order of 10^{-6} cm/s. The values of effective diffusion coefficient can be used to calculate the pre-exponential constant D_0, energy of activation E_a, and entropy of activation $\Delta S^{\#}$ by plotting it against $1/T$ using the following equations [45]:

$$D_i = D_0 \exp(-E_a/RT) \tag{14}$$

$$D_0 = (2.72\ d^2\ kT/h)\ \exp(\Delta S^{\#}/R) \tag{15}$$

The straight line graph obtained for the plot of D_i against $1/T$ permits the application of Arrhenius equation for the estimation of D_0 and E_a from the slope and intercept of the graph (Figure not shown) using Eq. (14). D_0 values are further used to calculate the entropy of activation using Eq. (15). The values of D_0, E_a, and $\Delta S^{\#}$ were estimated to be 6.4×10^{-8} cm^2 s^{-1}, 5.89 kJ/mol and -242.26 JK^{-1}/mol, respectively. The negative value of $\Delta S^{\#}$ furnished that no remarkable change has been observed in the internal structure of the modified wheat husk during adsorption of AO-10 [7].

3.11. Adsorption isotherms

Investigation of adsorption isotherm is important as it helps in understanding the interaction between adsorbate and adsorbent. The well known isotherm models namely Langmuir [46], Freundlich [47], and Dubinin–Radushkevich [48] isotherms were used to represent the equilibrium sorption data.

Linearized form of the Langmuir equation expressed as:

$$C_e/q_e = 1/Q_{max}b + C_e/Q_{max} \tag{16}$$

Linearized Freundlich model formulated as

$$\log q_e = \log K_F + 1/n\ \log C_e \tag{17}$$

Linearized form of Dubinin–Radushkevich isotherm model can be expressed as:

$$\ln q_e = \ln q_m - \beta\varepsilon^2 \tag{18}$$

$$E = 1/(2\beta)^{0.5} \tag{19}$$

where C_e (mg/L), q_e (mg/g) are the concentrations of adsorbate and amount of adsorbate adsorbed at equilibrium, respectively. The constant b (L/mg) is the Langmuir equilibrium constant and Q_{max} gives the theoretical monolayer saturation capacity. K_F (mg/g) is the Freundlich constant and n is the Freundlich exponent. The constant K_F is related to the degree of adsorption, $1/n$ provides the tentative estimation of the intensity of the adsorption, q_m is the theoretical monolayer saturation capacity (mg/g), β is the D–R model constant (mol^2/kJ^{-2}), and ε, is the Polanyi potential. The parameter β of D–R isotherm also gives an idea about the nature of sorption process using the relationship given in Eq. (22). For adsorption with E values between 1.0 and 8.0 kJ/mol the adsorbate–adsorbent interaction controlled by physical phenomenon and the sorption process proceed via ion exchange if values of E is between 8.0 and 16.0 kJ/mol [49].

The parameters of the isotherms were calculated and the values were given in Table 2. Langmuir, Freundlich, and D–R isotherm profile plotted between C_e/q_e and C_e, log q_e and log C_e ln q_e, and ε^2, respectively, at all three temperatures. The suitability of the isotherm model that agrees well with the experimental sorption data was predicted on the basis of correlation coefficient values and error analysis. The use of error analysis helps in determining the difference between the calculated parameter values from linear and nonlinear equations. The smaller values of error analysis indicating minimum difference between values calculated from linear and nonlinear equations. The present study uses statistical parameter χ^2 test for error analysis. The χ^2 test is principally the sum of the squares of differences between the experimental data and calculated data, with each squared difference divided by the corresponding data obtained by calculation from models. The model can be represented as [49]:

$$\chi^2 = \sum\{(q_{e,exp} - q_{e,cal})^2/(q_{e,exp})\} \tag{20}$$

where $q_{e,exp}$ and $q_{e,cal}$ are the experimental value and calculated value in mg/g, respectively. If the data from the model are similar to the experimental data

Table 3
Adsorption isotherm constants for sorption of AO-10 onto modified wheat husk at different temperatures

Dye	Model	30°C	40°C	50°C
Acid Orange 10	*Langmuir*			
	Q_{max} (mg/g)	31.29	29.41	25.64
	b (L/mg)	0.624	0.581	0.542
	R_L	0.021	0.022	0.024
	R^2	0.947	0.962	0.988
	χ^2	19.8	23.4	21.7
	Freundlich			
	K_F (mg/g)(L/mg)$^{1/n}$	7.095	3.862	3.17
	n	3.125	1.867	1.714
	R^2	0.988	0.999	0.999
	χ^2	0.037	0.062	0.084
	Dubinin–Radushkevich			
	q_m (mg/g)	25.13	12.58	9.24
	β (mol^2/kJ^{-2})	0.102	0.186	0.242
	E (kJ/mol)	2.22	1.66	1.45
	R^2	0.989	0.899	0.904
	χ^2	93.33	86.72	90.24

then value of χ^2 will be smaller and if they are different, χ^2 value will be large. The values of χ^2 for all isothermal studies were depicted in Table 3

The isotherm plot of Langmuir (Fig. 12) and D–R (Fig. 13) reflect poor linearity with low correlation coefficient values and high χ^2 values, indicated that the models were inappropriate in predicting sorption isotherm data. Moreover, the E values calculated from D–R plots signify that the nature of dye sorption controlled by physical process as the values evaluated for all the temperatures were found to be <8 kJ mol^{-1}. The Freundlich plots (Fig. 14) bear straight lines with high correlation coefficient values ($R^2 > 0.99$) and low χ^2 values clearly imply that the model satisfactorily fit the experimental equilibrium sorption data. These findings also infer that the adsorption of AO-10 by the modified wheat husk was multilayer type. The n value of Freundlich isotherm also provides an insight about the favorability of sorption process. If the magnitude of n estimated between 1 and 10 the sorption process considered to be favorable. For the present study, the values of n settled between 1 and 3 which reflects good adsorption characteristics of AO-10. The decrease of n values with temperature suggests that dye sorption is exothermic in nature.

3.12. Adsorption thermodynamics

The changes in Gibbs free energy (ΔG), enthalpy (ΔH), and entropy (ΔS) for the adsorption process were obtained using the following equations [50,51]:

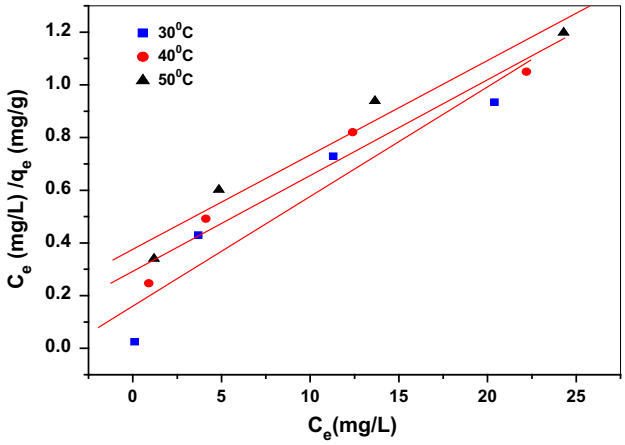

Fig. 12. Langmuir isotherm plot at different temperatures (adsorbent dose 2.5 g/L, pH 2, agitation speed 200 rpm).

$$\Delta G = -RT \ln b \quad (21)$$

$$\ln b = (\Delta S/R) - (\Delta H/RT) \quad (22)$$

where R is the ideal gas constant (kJ/mol K) and T is the temperature (K). The enthalpy change (ΔH) and the entropy change (ΔS) are calculated from a plot of ln$b$ (from Langmuir isotherm) vs. $1/T$ (figure not shown). The values calculated for Gibbs free energy at 303, 313, and 323 K were −10.2, −9.0 and −7.8 kJ/mol, respectively, indicates that adsorption process is spontaneous in nature and increase in negative values

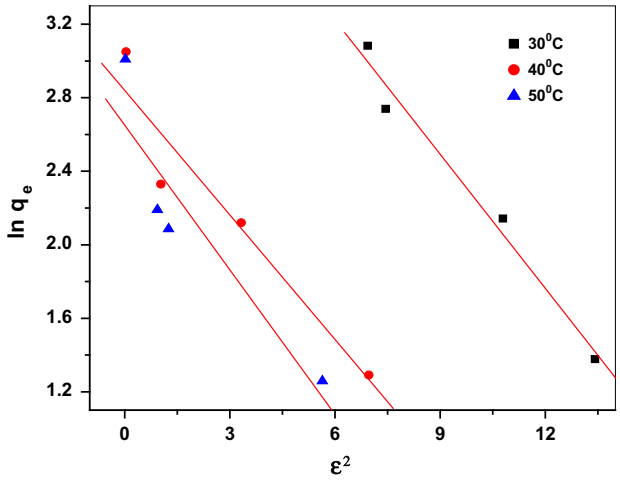

Fig. 13. D–R isotherm plot at different temperatures (adsorbent dose 2.5 g/L, pH 2, agitation speed 200 rpm).

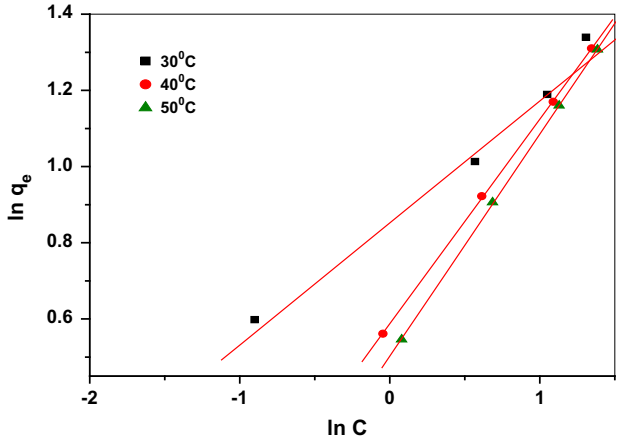

Fig. 14. Freundlich isotherm plot at different temperatures (adsorbent dose 2.5 g/L, pH 2, agitation speed 200 rpm).

of ΔG with decreasing temperature advocates adsorption was rapid and more favorable at low temperature. The negative value of ΔH (−20.7 kJ/mol) indicates that overall dye sorption process is exothermic in nature. The negative value of ΔS (−124.4 J/mol K) recommends that the disorder at the solid–liquid interface decreased during adsorption of AO-10 ions. The results of thermodynamic studies can also be used for predicting the nature of adsorption process. For the adsorption process if it was governed by physical sorption mechanism the values of ΔG should be in the range of −20 to 0 kJ/mol and the ΔH values must lie between 2.1 and 20.9 kJ/mol. In the present study, the calculated values of ΔG and ΔH found to be lie within the range of physical sorption process. Therefore, for present dye-adsorbent system physical interaction plays key role in sorption process.

3.13. Desorption studies

For desorption studies 0.25 g of AO-10-loaded saturated adsorbent was suspended in 100 mL of three different types of desorption solution namely 0.1 M CH_3COOH, 0.1 M HCl and 0.1 M NaOH, and agitate for 2 h at 303 K. The suspended products then separated from the liquid phase by centrifugation followed by washing liberally and oven dried at 80˚C for overnight. The dried material was then examined for adsorption capacity. The supernatant left after centrifugation was analyzed spectrophotometrically. The experimental results suggest that maximum desorption of 86.3% occurred when NaOH was used as desorption solution followed by CH_3COOH leads to desorption of 64.7%, and lowest desorption of 37.4% was observed when HCl was used as a desorption solution. The reaction that might occur using NaOH for desorption studies given as:

$$\text{Ce-OH}_2^+\text{SO}_3^- - \text{Dye} + \text{NaOH} \xrightarrow{\text{desorption}} \text{Ce-OH} + \text{Dye} - \text{SO}_3\text{Na} + \text{H}_2\text{O} \quad (23)$$

The adsorption competency founds to be unaltered up to second reuse cycle after that adsorbent loses its efficiency remarkably. The adsorption efficiency of the adsorbent up to second cycle was more than 80%, and after that the adsorption capacity tumbled down to below 60%. The above results recommend that the recycled adsorbent can be effectively used for two consecutive studies. The reuse of the adsorbent will also help in reducing amount of sludge generation in the removal process.

4. Conclusion

The wheat husk after modification has been used for the removal of anionic dye AO-10 from aqueous solutions. The characterization results infer that perchloric acid treatment modifies the adsorbent significantly with enhanced porosity. The maximum removal of dye was observed at pH 2.0. The percentage dye removal was found to be increased with the contact time, adsorbent dosage, and ionic strength (NaCl) of the solution. However, it was also observed dye removal percentage diminished slightly with the increase in initial dye concentration and temperature.

The investigation of adsorption kinetics suggest that experimental data agreed reasonably with pseudo-second-order kinetics and sorption process is controlled by external diffusion. The study of adsorption isotherm reveals that Freundlich isotherm model better represents the equilibrium sorption data than that of Langmuir and D–R model. The study of adsorption thermodynamics indicates that dye sorption process is spontaneous and exothermic in nature and the interaction between dye and adsorbent is governed by physical forces. Desorption study furnished that adsorbent can be effectively reused for two consecutive times before disposal.

Acknowledgment

One of the authors (SB) is thankful to CSIR, New Delhi, for awarding SRF.

References

[1] M.T. Yagub, T.K. Sen, S. Afroze, H.M. Ang, Dye and its removal from aqueous solution by adsorption: A review, Adv. Colloid Interface Sci. 209 (2014) 172–184.
[2] S. Banerjee, Uma, M.C. Chattopadhyaya, Y.C. Sharma, Fast and economically viable removal of a cationic dye from aqueous solutions: Kinetic and equilibrium modeling, Environ. Eng. Manag. J. 12 (2013) 2183–2190.
[3] Y. Feng, D.D. Dionysiou, Y. Wu, H. Zhou, L. Xue, S. He, L. Yang, Adsorption of dyestuff from aqueous solutions through oxalic acid-modified swede rape straw: Adsorption process and disposal methodology of depleted bioadsorbents, Bioresour. Technol. 138 (2013) 191–197.
[4] Y. Wong, Y. Szeto, W. Cheung, G. McKay, Adsorption of acid dyes on chitosan—Equilibrium isotherm analyses, Process Biochem. 39 (2004) 693–702.
[5] M. Ghaedi, H. Hossainian, M. Montazerozohori, A. Shokrollahi, F. Shojaipour, M. Soylak, M.K. Purkait, A novel acorn based adsorbent for the removal of brilliant green, Desalination 281 (2011) 226–233.
[6] V.K. Gupta, A. Mittal, L. Krishnan, V. Gajbe, Adsorption kinetics and column operations for the removal and recovery of malachite green from wastewater using bottom ash, Sep. Purif. Technol. 40 (2004) 87–96.
[7] A. Mittal, L. Krishnan, V.K. Gupta, Removal and recovery of malachite green from wastewater using an agricultural waste material, de-oiled soya, Sep. Purif. Technol. 43 (2005) 125–133.
[8] A. Mittal, Adsorption kinetics of removal of a toxic dye, Malachite Green, from wastewater by using hen feathers, J. Hazard. Mater. 133 (2006) 196–202.
[9] A. Mittal, L. Kurup, Column operations for the removal and recovery of a hazardous dye 'acid red - 27' from aqueous solutions, using waste materials - bottom ash and de-oiled soya, Ecol. Environ. Conserv. 13 (2006) 181–186.
[10] A. Mittal, Removal of the dye, amaranth from waste water using hen feathers as potential adsorbent, Electron J. Environ. Agri. Food Chem. 5 (2006) 1296–1305.
[11] A. Mittal, V. Thakur, V. Gajbe, Adsorptive removal of toxic azo dye Amido Black 10B by hen feather, Environ. Sci. Pollut. Res. 20 (2013) 260–269.
[12] J. Mittal, V. Thakur, A. Mittal, Batch removal of hazardous azo dye Bismark Brown R using waste material hen feather, Ecol. Eng. 60 (2013) 249–253.
[13] S. Banerjee, V. Nigam, R.K. Gautam, S. Halder, M.C. Chattopadhyaya, Removal of anionic dye, Orange G from aqueous solutions by adsorption on unmodified sheesham (*Dalbergia sisso*) saw dust, J. Indian Chem. Soc. 90 (2013) 555–563.
[14] R.K. Gautam, A. Mudhoo, M.C. Chattopadhyaya, Kinetic, equilibrium, thermodynamic studies and spectroscopic analysis of Alizarin Red S removal by mustard husk, J. Environ. Chem. Eng. 1 (2013) 1283–1291.
[15] A. Mittal, V. Thakur, J. Mittal, H. Vardhan, Process development for the removal of hazardous anionic azo dye Congo red from wastewater by using hen feather as potential adsorbent, Desalin. Water Treat. 52 (2014) 227–237.
[16] H. Daraei, A. Mittal, J. Mittal, H. Kamali, Optimization of Cr (VI) removal onto biosorbent eggshell membrane: Experimental & theoretical approaches, Desalin. Water Treat. 52(7–9) (2014) 1307–1315.
[17] J. Mittal, D. Jhare, H. Vardhan, A. Mittal, Utilization of bottom ash as a low-cost sorbent for the removal and recovery of a toxic halogen containing dye eosin yellow, Desalin. Water Treat. 52 (2014) 4508–4519.
[18] G. Sharma, M. Naushad, D. Pathania, A. Mittaland, G.E. El-desoky, Modification of *Hibiscus cannabinus* fiber by graft copolymerization: application for dye removal, Desalin. Water Treat. (2014) 1–8, doi: 10.1080/19443994.2014.904822.
[19] M.E. Argun, S. Dursun, C. Ozdemir, M. Karatas, Heavy metal adsorption by modified oak sawdust: Thermodynamics and kinetics, J. Hazard. Mater. 141 (2007) 77–85.
[20] Y. Bulut, H. Aydın, A kinetics and thermodynamics study of methylene blue adsorption on wheat shells, Desalination 194 (2006) 259–267.
[21] S. Banerjee, M.C. Chattopadhyaya, Uma, Y.C. Sharma, Adsorption characteristics of modified wheat husk for the removal of a toxic dye, methylene blue, from aqueous solutions, J. Hazard. Toxic Radioactive Wastes 18 (2014) 56–63.
[22] A.K. Giri, A. Mukherjee, G. Talukder, A. Sharma, In vivo cytogenetic studies on mice exposed to Orange G, a food colourant, Toxicol. Lett. 44 (1988) 253–261.
[23] I.F. Gaunt, I.S. Kiss, P. Grasso, S.D. Gangolli, Short-term toxicity of orange G in pigs, Food and Cosmetics Toxicol. 11 (1973) 367–374.
[24] N.-H. Benselka-Hadj Abdelkader, A. Bentouami, Z. Derriche, N. Bettahar, L.-C. de Ménorval, Synthesis and characterization of Mg–Fe layer double hydroxides and its application on adsorption of Orange G from aqueous solution, Chem. Eng. J. 169 (2011) 231–238.
[25] Y.P. Guo, D.A. Rockstraw, Physical and chemical properties of carbons synthesized from xylan, cellulose, and Kraft lignin by H3PO4 activation, Carbon 44 (2006) 1464–1475.

[26] A.K. Bledzki, A.A. Mamun, N.N. Bonnia, S. Ahmad, Basic properties of grain by-products and their viability in polypropylene composites, Ind. Crops. Prod. 37 (2012) 427–434.
[27] J.C. del Río, A. Gutiérrez, I.M. Rodríguez, D. Ibarra, Ángel T. Martínez, Composition of non-woody plant lignins and cinnamic acids by Py-GC/MS, Py/TMAH and FT-IR, J. Anal. Appl. Pyrolysis 79 (2007) 39–46.
[28] W.T. Tsai, H.R. Chen, Removal of malachite green from aqueous solution using low-cost chlorella-based biomass, J. Hazard. Mater. 175 (2010) 844–849.
[29] S. Chowdhury, S. Chakraborty, P. Saha, Biosorption of basic green 4 from aqueous solution by *Ananas comosus* (pineapple) leaf powder, Coll. Surf. B 84 (2011) 520–527.
[30] S. Chatterjee, S. Chatterjee, B.P. Chatterjee, A.K. Guha, Adsorptive removal of congo red, a carcinogenic textile dye by chitosan hydrobeads: Binding mechanism, equilibrium and kinetics, Colloids Surf., A 299 (2007) 146–152.
[31] H. Demir, A. Top, D. Balköse, S. Ülkü, Dye adsorption behavior of Luffa cylindrica fibers, J. Hazard. Mater. 153 (2008) 389–394.
[32] A. Altınışık, E. Gür, Y. Seki, A natural sorbent, Luffa cylindrica for the removal of a model basic dye, J. Hazard. Mater. 179 (2010) 658–664.
[33] S. Rovani, A.N. Fernandes, L.D.T. Prola, E.C. Lima, W.O. Santos, M.A. Adebayo, Removal of cibacron brilliant yellow 3G-P dye from aqueous solutions by Brazilian peats as biosorbents, Chem. Eng. Commun. 201 (2014) 1431–1458.
[34] Y.S. Al-Degs, M.A.M. Khraisheh, S.J. Allen, M.N. Ahmad, Adsorption characteristics of reactive dyes in columns of activated carbon, J. Hazard. Mater. 165 (2009) 944–949.
[35] H. Daraei, A. Mittal, M. Noorisepehr, J. Mittal, Separation of chromium from water samples using eggshell powder as a low-cost sorbent: Kinetic and thermodynamic studies, Desalin. Water Treat. 53 (2015) 214–220.
[36] S. Lagergren, About the theory of so-called adsorption of soluble substances, K. Sven. Vetenskapsakad. Handl. 244 (1898) 1–39.
[37] Y.S. Ho, Pseudo-isotherms using a second order kinetic expression constant, Adsorption 10 (2004) 151–158.
[38] W.J. Weber, J.C. Morris, Kinetics of adsorption on carbon from solution, J. Sanit. Eng. Div. Am. Soc. Civ. Eng. 89 (1963) 31–60.
[39] R.K. Gautam, P.K. Gautam, S. Banerjee, V. Rawat, S. Soni, S.K. Sharma, M.C. Chattopadhyaya, Removal of tartrazine by activated carbon biosorbents of *Lantana camara*: Kinetics, equilibrium modeling and spectroscopic analysis, J. Environ. Chem. Eng. 3 (2015) 79–88.
[40] V.C. Srivastava, I.D. Mall, I.M. Mishra, Characterization of mesoporous rice husk ash (RHA) and adsorption kinetics of metal ions from aqueous solution onto RHA, J. Hazard. Mater. 134 (2006) 257–267.
[41] G. McKay, S.J. Allen, I.F. McConvey, M.S. Otterburn, Transport processes in the sorption of colored ions by peat particles, J. Colloid Interface. Sci. 80 (1981) 323–339.
[42] G.E. Boyd, A.W. Adamson, L.S. Myers, The exchange adsorption of ions from aqueous solutions by organic zeolites. II. kinetics 1, J. Am. Chem. Soc. 69 (1947) 2836–2848.
[43] D. Reichenberg, Properties of ion-exchange resins in relation to their structure. III. kinetics of exchange, J. Am. Chem. Soc. 75 (1953) 589–597.
[44] N.K. Goel, V. Kumar, S. Pahan, Y.K. Bhardwaj, S. Sabharwal, Development of adsorbent from Teflon waste by radiation induced grafting: Equilibrium and kinetic adsorption of dyes, J. Hazard. Mater. 193 (2011) 17–26.
[45] M. Naushad, A. Mittal, M. Rathore, V. Gupta, Ion-exchange kinetic studies for Cd (II), Co (II), Cu (II), and Pb (II) metal ions over a composite cation exchanger, Desalin. Water Treat. 54 (2015) 2883–2890, doi: 10.1080/19443994.2014.904823.
[46] I. Langmuir, The constitution and fundamental properties of solids and liquids. Part I. Solids, J. Am. Chem. Soc 38 (1916) 2221–2295.
[47] H.M.F. Freundlich, Over the adsorption in solution, J. Phys. Chem. 57 (1906) 385–470.
[48] M. M.Dubinin, E.D. Zaverina, L.V. Radushkevich, Sorption and structure of activated carbons. I. Adsorption of organic vapours, J. Phy. Chem. 21 (1947) 1351–1362.
[49] M. Rajiv Gandhi, N. Viswanathan, S. Meenakshi, Preparation and application of alumina/chitosan biocomposite, Int. J. Bio. Macromolecules 47 (2010) 146–154.
[50] S. Banerjee, G.C. Sharma, M.C. Chattopadhyaya, Y.C. Sharma, Kinetic and equilibrium modeling for the adsorptive removal of methylene blue from aqueous solutions on of activated fly ash (AFSH), J. Env. Chem. Eng. 2 (2014) 1870–1880.
[51] R. Jain, P. Sharma, S. Sikarwar, J. Mittal, D. Pathak, Adsorption kinetics and thermodynamics of hazardous dye Tropaeoline 000 unto Aeroxide Alu C (Nano alumina): A non-carbon adsorbent, Desalin. Water Treat. 52 (2014) 7776–7783.